ChemComm

COMMUNICATION

View Article Online
View Journal | View Issue

Cite this: *Chem. Commun.*, 2023, 59, 6243

Received 9th March 2023,
Accepted 24th April 2023

DOI: 10.1039/d3cc01187a

rsc.li/chemcomm

Electrophilic and nucleophilic gas phase reactivity of the Janus cluster-based anions $[\{Mo_6Cl_8\}Cl_5\square]^-$ ($\square$ = lacuna)†

Antoine Denis,[a] Nina Tymínska,[b] Thomas Delhaye,[a] Yann Molard,[b] Pascal Gerbaux,[c] Julien De Winter,[c] Mohamed Himdi,[a] Xavier Castel,[a] Karine Costuas,*[b] Stéphane Cordier*[b] and David Rondeau*[a]

The lacunary monocharged anion $[\{Mo_6Cl_8^i\}Cl_5^a\square^a]^-$ presents concomitantly a strongly electrophilic site and a nucleophilic one. This Janus character in terms of reactivity is confirmed by its gas phase reaction with $[Br_6Cs_4K]^-$ to form $[\{Mo_6Cl_8^i\}Cl_5^aBr^a]^{2-}$ and by its unusual self-reactivity leading to $[\{Mo_6Cl_8^i\}Cl_6^a]^{2-}$ dianions.

Cluster-based ternary halides of general formula $A_2[\{Mo_6X_8^i\}X_6^a]$ (A = Cs^+, Rb^+, K^+; X = Cl, Br or I; inner ligand "i", apical ligand "a") ($[\{Mo_6X_8^i\}X_6^a]^{2-}$ depicted in Scheme 1) are prepared by solid-state chemistry at high temperature. Contrary to many other inorganic solid-state compounds, the $A_2[\{Mo_6X_8^i\}X_6^a]$ halides are soluble in acidified aqueous solution and in common organic solvents, which allows their facilitated integration in functional materials. In all these materials, the $[\{Mo_6X_8^i\}X_6^a]^{2-}$ cluster units or their derivatives (obtained by ligand substitutions) are the active species, which experience during integration bond energy activations, nucleation processes, chemical reactions or electronic excitations and further processes. These numerous and various properties (photoluminescence, (photo-)(electro-) catalysis, light harvesting properties) open the way for a wide range of potential applications in the field of display and lighting technologies, sustainable energy and health.[1,2] This is thus of prime interest to study the intrinsic properties and reactivities of discrete cluster units in order to perform the rational design and elaboration of materials.[3–5] Some gas phase studies of $[\{Mo_6X_8^i\}X_6^a]^{2-}$ dianions (X = Cl, Br and I) have been recently conducted using collision-induced dissociation (CID) mass spectrometry (MS) measurements and quantum chemical calculations.[6] In particular, the fragmentation pathways initiated by the loss of an X^- anion, and the sequential eliminations of MoX_2 and $X^\bullet$ radicals have been described. The propensity of fragment ions to form O_2 or H_2O adducts has also been highlighted.

In the present work, we demonstrate that the weakly nucleophilic monocharged $[\{Mo_6Cl_8^i\}Cl_5^a\square^a]^-$ ($\square$ = lacuna) anions prepared in the gas phase from $[\{Mo_6Cl_8^i\}Cl_6^a]^{2-}$ by a Cl^{a-} ligand loss represent one of the few examples of anionic electrophiles. Surprisingly, we observed that these negatively-charged electrophilic ions readily react in the gas phase with $\{Cs_4KBr_6\}^-$ anions by bromine abstraction, despite the coulombic repulsion. Quantum chemical studies of the isolated $[\{Mo_6Cl_8^i\}Cl_5^a\square^a]^-$ have been combined with MS experiments to secure the interpretation. These results are compared and discussed with those reported for $[B_{12}L_{11}]^-$ (L = F, Cl, I or CN) superelectrophilic anions.[7–11]

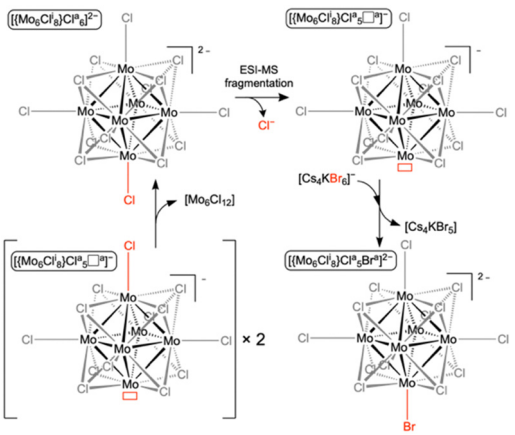

Scheme 1 Description of the ESI-MS fragmentation process of $[\{Mo_6Cl_8^i\}Cl_6^a]^{2-}$ leading to $[\{Mo_6Cl_8^i\}Cl_5^a\square^a]^-$; reactivity of $[\{Mo_6Cl_8^i\}Cl_5^a\square^a]^-$ with $[Cs_4KBr_6]^-$; $[\{Mo_6Cl_8^i\}Cl_5^a\square^a]^-$ self-reactivity.

[a] *Univ Rennes, CNRS, Institut d'Electronique et des Technologies du numéRique – UMR 6164, Rennes F-35000, France. E-mail: david.rondeau@univ-rennes.fr*
[b] *Univ Rennes, Institut des Sciences Chimiques de Rennes – UMR 6226, Rennes F-35000, France. E-mail: karine.costuas@univ-rennes.fr, stephane.cordier@univ-rennes.fr*
[c] *Organic Synthesis and Mass Spectrometry Laboratory, Interdisciplinary Center for Mass Spectrometry (CISMa), University of Mons – UMONS, 23 Place du Parc, Mons 7000, Belgium*

† Electronic supplementary information (ESI) available: Syntheses, experimental and computational details, MS spectra. See DOI: https://doi.org/10.1039/d3cc01187a

Table 1 Calculated heterolytic Mo–Cl^a bonding dissociation energies ΔE_{bond} in $[\{Mo_6Cl^i_8\}Cl^a_5\square^a]^-$ and $[\{Mo_6Cl^i_8\}Cl^a_6]^{2-}$ (in eV). The energy decomposition is given in terms of fragment distorsion energy (ΔE_{prep}), Pauli repulsion (ΔE_{Pauli}), electrostatic (ΔE_{elstat}), orbital interactions (ΔE_{orb}), dispersion (ΔE_{disp}), and basis set superposition error correction (ΔE_{BSSE}).[12–17] Zero-point vibrational corrections are not included

	$[\{Mo_6Cl^i_8\}Cl^a_5\square^a]^-$	$[\{Mo_6Cl^i_8\}Cl^a_6]^{2-}$
ΔE_{prep}	0.282	0.083
ΔE_{Pauli}	4.163	5.222
ΔE_{elstat}	−2.303	−5.357
ΔE_{orb}	−2.696	−3.291
ΔE_{disp}	−0.375	−0.395
ΔE_{BSSE}	0.030	0.030
ΔE_{bond} (in kJ mol^{-1})	−0.898 (−86.6)	−3.708 (−357.7)

Geometry optimizations and the subsequent computational studies were performed at the DFT level (see ESI† for details). The Mo–Cl^a heterolytic bond dissociation energies (ΔE_{bond}) were calculated for $[\{Mo_6Cl^i_8\}Cl^a_5\square^a]^-$ and $[\{Mo_6Cl^i_8\}Cl^a_6]^{2-}$ cluster units. The Mo–Cl^a ΔE_{bond} values in $[\{Mo_6Cl^i_8\}Cl^a_6]^{2-}$ ($[\{Mo_6Cl^i_8\}Cl^a_5\square^a]^-$ + Cl^-) and in $[\{Mo_6Cl^i_8\}Cl^a_5\square^a]^-$ (*trans*-$[\{Mo_6Cl^i_8\}Cl^a_4\square^a_2]^-$ + Cl^-) were determined by an energy decomposition analysis, as reported in Table 1. This highlights the iono-covalent character of the Mo–Cl^a bonds, for which the main component is electrostatic. The latter is much stronger in $[\{Mo_6Cl^i_8\}Cl^a_6]^{2-}$ than in $[\{Mo_6Cl^i_8\}Cl^a_5\square^a]^-$. It is apparently counterintuitive since the two fragments resulting from the bond cleavage in $[\{Mo_6Cl^i_8\}Cl^a_6]^{2-}$, *i.e.* Cl^- and $[\{Mo_6Cl^i_8\}Cl^a_5\square^a]^-$, are negatively charged and should generate electrostatic repulsions when interacting. Mapping the computed electrostatic potential of $[\{Mo_6Cl^i_8\}Cl^a_5\square^a]^-$ reveals its non-uniform distribution with alternation of positive and negative potentials on the Mo and Cl atoms, respectively (Fig. 1). Thus, if a negatively-charged reactant is approaching along the dipole moment axis of $[\{Mo_6Cl^i_8\}Cl^a_5\square^a]^-$, an electrostatic attraction will occur since the Mo atom bearing the lacuna is strongly positively charged even though the molecule is globally negatively-charged. Interestingly, the most negative regions are located around the five apical ligands (Cl^a).

The visualization of the Fukui functions for electrophilic (f^+) and nucleophilic (f^-) attacks represented in Fig. 1 unambiguously prove the Janus character of $[\{Mo_6Cl^i_8\}Cl^a_5\square^a]^-$. Indeed, it is sensitive to electrophilic attack on the Cl ligand in the *trans* position to the lacuna of Cl^-, and at the same time the Mo atom without an apical ligand is highly sensitive to nucleophilic attack.[18] It has to be emphasized that these two reactive sites are positioned on the dipole moment axis. The calculated Gibbs free energy of the reaction $2 \times [\{Mo_6Cl^i_8\}Cl^a_5\square^a]^- \rightarrow [\{Mo_6Cl^i_8\}Cl^a_4\square^a_2]^0 + [\{Mo_6Cl^i_8\}Cl^a_6]^{2-}$ is 263 kJ mol^{-1} at 298 K, which is thermodynamically accessible considering the kinetic energies of the ions subjected to an applied electric field (as in the MS experiment described below). It has to be noted that the calculations of bonding and total energies for the $[Br_6Cs_4K]^-$ ion could not be considered in the present study since structural information is lacking. Several tens of possible geometrical arrangements could be envisioned and would be the subject of a computational study on their own.

The $[\{Mo_6Cl^i_8\}Cl^a_6]^{2-}$ dianion has been identified by negative ion mode electrospray ionization high resolution MS (ESI-HRMS) analysis of a $Cs_2[\{Mo_6Cl^i_8\}Cl^a_6]$ acetonitrile solution as proved by the high resolution mass spectrum given in Fig. S1 (ESI†). Indeed, the latter shows an isotopic distribution centered at *m*/*z* 535.5 that perfectly matches the theoretical isotopic distribution of a Mo_6Cl_{14} dianion (see ESI† for details). A second isotopic pattern centered at *m*/*z* 1036.0 is observed. It corresponds to the formation of monocharged $[Mo_6Cl_{13}]^-$ ions that result from the loss of a Cl^- ligand from $[\{Mo_6Cl^i_8\}Cl^a_6]^{2-}$. This in-source collision induced dissociation (CID) occurs in the desolvation interface that separates the atmospheric pressure of the ESI-MS source from the analyzer vacuum of the Waters Synapt G2-Si mass spectrometer. This phenomenon has already been reported for the $[\{Mo_6X^i_8\}X^a_6]^{2-}$ ions.[6]

Second-generation fragment ions are further produced in the course of CID experiments from the in-source-generated $[\{Mo_6Cl^i_8\}Cl^a_5\square^a]^-$ fragment ions by selecting the whole isotopic pattern centered at *m*/*z* 1036. Surprisingly, as revealed by the CID mass spectrum shown in Fig. 2, $[\{Mo_6Cl^i_8\}Cl^a_6]^{2-}$ ions are produced and seem to arise from a chlorine ion addition to the mass-selected $[\{Mo_6Cl^i_8\}Cl^a_5\square^a]^-$.

The formation of these $[\{Mo_6Cl^i_8\}Cl^a_6]^{2-}$ ions can only be explained based on a bimolecular interaction between two $[\{Mo_6Cl^i_8\}Cl^a_5\square^a]^-$ ions concomitantly present in the T-wave (traveling wave) collision cell, as described in Scheme 1.

To confirm this, complementary MS experiments were performed. First, a solution of $Cs_2[\{Mo_6Cl^i_8\}Cl^a_6]$ and cesium

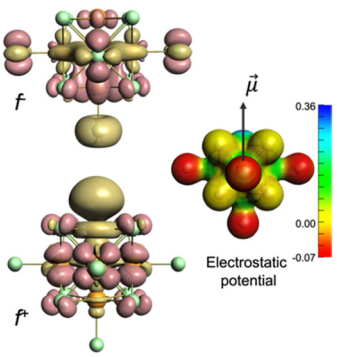

Fig. 1 Left: Fukui functions for electrophilic (f+) and nucleophilic (f−) attack (±0.001 au) of $[\{Mo_6Cl^i_8\}Cl^a_5\square^a]^-$. Right: Electrostatic potential (in Hartree) mapped onto the isodensity (±0.03 e Bohr^{-3}); representation of the dipole moment $\vec{\mu}$ (6.52 Debye) by an arrow (origin = Mo_6 centre).

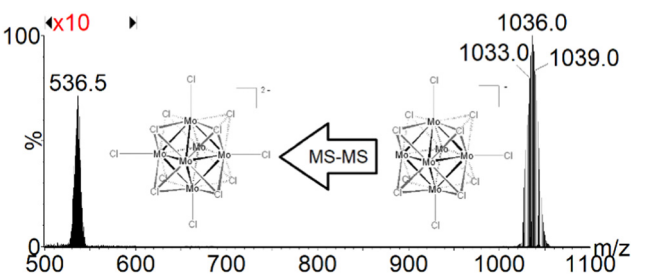

Fig. 2 Negative ESI-MS-MS spectrum of the $[Mo_6Cl_{13}]^-$ ion selected in a mass range encompassing an experimental isotopic pattern centered at *m*/*z* 1036. Signal magnification of 10 times in *m*/*z* 500–800.

bromide, CsBr, in acetonitrile was submitted to ESI-MS analysis (see ESI† for details). A full-scan ESI-MS spectrum of the solution in negative ion mode is presented in Fig. 3. Beside the most abundant $[\{Mo_6Cl_8^i\}Cl_6^a\square^a]^{2-}$ ions, additional anions were detected. *m/z* 718.4 and 930.2 ions are characteristic of adducts produced in the gas-phase by ESI-MS of cesium bromide in solution. More interesting is the detection of abundant *m/z* 558.5 ions that are readily ascribed to $[Mo_6Cl_{13}Br]^{2-}$ ions. The observation of these Cl^- and Br^--containing ions suggests that a ligand-exchange reaction occurred between $[Mo_6Cl_{13}]^-$ and Br^--containing ions. At this stage of the study, we can of course not define whether this reaction is occurring in solution or in the gaseous ion beam.

Furthermore, taking advantage of the fact that $[Cs_4KBr_6]^-$ ions and $[Mo_6Cl_{13}]^-$ are characterized by proximal *m/z* values, with their isotopic patterns overlapping in the *m/z* 970–1070 range, these anions may be concomitantly mass-selected in the course of CID experiments by enlarging the quadrupole mass selection window, *i.e.* from *m/z* 1010 to *m/z* 1070. The resulting mass spectrum that is represented in Fig. 4 shows not only the generation of the $[\{Mo_6Cl_8^i\}Cl_6^a]^{2-}$ ions (*i.e.* chlorine addition on the mass-selected ions) as observed previously when selecting only $[Mo_6Cl_{13}]^-$ ions, but also the formation of the halogen-mixed $[Mo_6Cl_{13}Br]^{2-}$ ions. We propose to attribute the formation of the $[\{Mo_6Cl_8^i\}Cl_6^a]^{2-}$ to the reactive self-interaction under collision activation of the $[Mo_6Cl_{13}]^-$ selected ions (Scheme 1). Similarly, the $[Mo_6Cl_{13}Br]^{2-}$ ions are likely to be issued from the reaction in the T-Wave™ cell of the mass spectrometer between $[\{Mo_6Cl_8^i\}Cl_5^a\square^a]^-$ and $[Cs_4KBr_6]^-$ ions, as described in Scheme 1. Besides the $[Mo_6Cl_{13}Br]^{2-}$ isotopic pattern centered on the *m/z* 558.5 value, other signals detected support this assumption (Fig. 4). If the ions at *m/z* 836.3 ($[Cs_3KBr_5]^-$, Fig. S2, ESI†), *m/z* 718.4 ($[Cs_3Br_4]^-$, Fig. S3, ESI†)

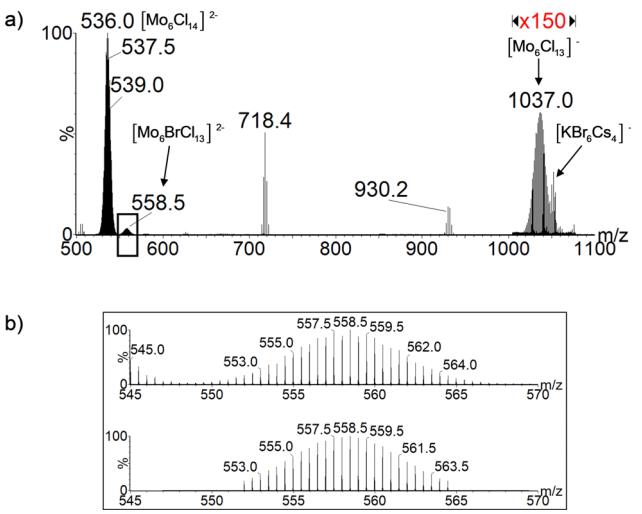

Fig. 3 (a) Negative ESI-MS full-scan MS spectrum of a solution of $Cs_2[\{Mo_6Cl_8^i\}Cl_6^a]$ and cesium bromide. A signal magnification of 150 times was done in the *m/z* 970–1070 range. The major signals at *m/z* 930.2 and 718.4 correspond to the $[Br_5Cs_4]^-$ and $[Br_4Cs_5]^-$, respectively. (b) Experimental (top) and theoretical (bottom) isotopic patterns of the $[Mo_6Cl_{13}Br]^{2-}$ ion (*m/z* 545–575).

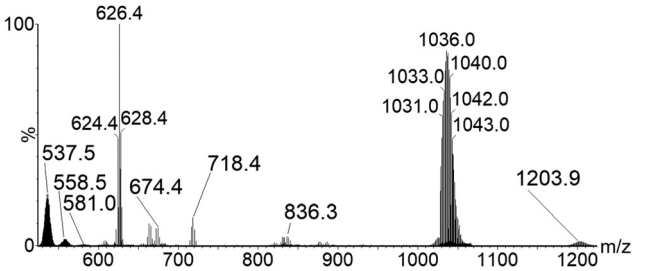

Fig. 4 Negative ESI-MS-MS spectrum of the $[Mo_6Cl_{13}]^-$ and $[Cs_4KBr_6]^-$ ions selected around *m/z* 1036 (see ESI† for more details).

and *m/z* 624.4 ($[Cs_2KBr_4]^-$, Fig. S4, ESI†) can be attributed to the dissociation of the selected $[Cs_4KBr_6]^-$ ion, the ions at *m/z* 674.4 ($[Cs_3Br_3Cl]^-$, Fig. S5, ESI†), *m/z* 628.5 ($[Cs_3Br_2Cl_2]^-$, Fig. S6, ESI†) and *m/z* 584.4 ($[Mo_6Cl_{12}Br_2]^{2-}$, Fig. S7, ESI†) are ionic species produced by Cl^- and Br^- exchanges between the concomitantly mass-selected two precursor ions. It is unlikely that halide exchanges would arise by an initial dissociation step of both $[Mo_6Cl_{13}]^-$ and $[Cs_4KBr_6]^-$ ions followed by Br^- capture by the former and the Cl^- capture by the fragments of the latter. $[Cs_3Br_2Cl_2]^-$ (*m/z* 628.5) and $[Mo_6Cl_{12}Br_2]^{2-}$ (*m/z* 584.4) ions could be observed if such processes occur. Finally, $[CsMo_6Cl_{14}]^-$ (Fig. S8, ESI†) whose isotopic pattern is observed around the *m/z* 1209.3 value (Fig. 4), involves the transfer of a Cs^+ cation and a Cl^- anion that can only be due to an interaction between $[Mo_6Cl_{13}]^-$ and $[Cs_4KBr_6]^-$ ions. It has to be noted that the ions produced by the halide exchanges during the collision activation are not detected anymore upon increasing the trap collision voltage to 5 V. This experiment unambiguously demonstrates that the reactions occur in the gaseous ion beam.

Gas phase nucleophilic addition reactions between anion clusters such as $[B_{12}L_{11}]^-$ (L = F, Cl, I or CN) and inert molecules such as argon, krypton, neon and N_2 have already been described in several MS experiments attesting to the electrophilic character of the anion clusters.[8–10] This behavior is attributed by the authors to a strong electronic density depletion at the active site, qualifying these ions as "dipole-discriminating electrophilic anions" on the basis of computational results.[10] More importantly, in the same family of compounds, $[B_{12}I_9]^-$ anions have been shown to dimerize within an ion trap collision cell giving rise to $[B_{24}I_{18}]^{2-}$ dianions.[19,20] These results unambiguously prove the possibility of interactions between anions in MS experiments.

In the present study, it is a bond breaking that is observed. Indeed, CID-MS-MS experiments show that Br^- is transferred from $[Cs_4KBr_6]^-$ to $[\{Mo_6Cl_8^i\}Cl_5^a\square^a]^-$ to yield $[\{Mo_6Cl_8^i\}Cl_5^aBr^a]^{2-}$. The reactivities of $[\{Mo_6Cl_8^i\}Cl_5^a\square^a]^-$ in tandem-in-space MS experiments and the dimerization of $[B_{12}I_9]^-$ anions in ESI-MS are counter-intuitive at first sight since the ion density is low and anions should repel each other considering that they are negatively-charged. In the present CID-MS-MS experiments, since the anions are moving in the same direction should additionally prevent interactions. A few studies of ion trajectories through high pressure quadrupole cell modelling are available.[21,22] Lock *et al.*[22] established that only the quadrupole collision cell becomes

thermalized in such experiments considering that ions are crossing a relatively high pressure radio frequency cell. Ions could thus exit the device *via* the repulsive effects between them while streaming into the entrance of the cell.

The clue comes from the study of the electrostatic and electronic features of the $[\{Mo_6Cl_8^i\}Cl_5^a\square^a]^-$ ions. As shown in the computational section, there is a heterogeneous distribution of positive and negative charges at the surface of the monocharged $[\{Mo_6Cl_8^i\}Cl_5^a\square^a]^-$ anions. The electronic density depletion observed around the lacunary molybdenum atom is similar to what is reported in the $[B_{12}L_{11}]^-$ series (see electrostatic potential mapping in Fig. 1). This allows concluding that no coulombic repulsion occurs if the interaction with a negatively-charged ion happens in the vicinity of the positively-charged parts of the $[\{Mo_6Cl_8^i\}Cl_5^a\square^a]^-$ cluster ions. Quantum chemical calculations reveal that the lacunary molybdenum site of the $[\{Mo_6Cl_8^i\}Cl_5^a\square^a]^-$ mono-anion is moreover highly sensitive to nucleophilic attacks (Fig. 1).

The detection of $[\{Mo_6Cl_8^i\}Cl_5^aBr^a]^{2-}$ species when isolating the $[\{Mo_6Cl_8^i\}Cl_5^a\square^a]^-$ and $[Cs_4KBr_6]^-$ species concomitantly reveals that the energy acquired by the ions is sufficient to subtract Br^- from $[Cs_4KBr_6]^-$. This leaves a neutral $[Cs_4KBr_5]$ entity, which cannot be detected by MS. Note that, due to the lack of structural data for the $[Cs_4KBr_6]^-$ ions, the energy requirement of the transfer reaction is not yet established, making the ion kinetic energy dependency on the Br^- transfer reaction efficiency still to be evaluated. Importantly, this result reveals that there is a confinement effect in the T-Wave™ cell or the travelling wave ion guide (TWIG) trap that is sufficient to allow ion interaction as already pointed out by Lock and coworkers in the case of high pressure cells.[21,22]

The same process is involved in the formation of $[\{Mo_6Cl_8^i\}Cl_6^a]^{2-}$, which consists in a heterolytic Mo–Cl bond breaking in $[\{Mo_6Cl_8^i\}Cl_5^a\square^a]-$ by interaction with a second $[\{Mo_6Cl_8^i\}Cl_5^a\square^a]^-$ ion. In that case, the required energy to subtract Cl^- from $[\{Mo_6Cl_8^i\}Cl_5^a\square^a]^-$ is estimated to be 263 kJ mol^{-1} by quantum chemical calculations. This is of the order of magnitude of what can be evaluated in terms of total internal energy imparted in the precursor ion during a collision process such as described in the present experiments (see ESI† for details). The computational study reveals that $[\{Mo_6Cl_8^i\}Cl_5^a\square^a]^-$ is indeed susceptible to electrophilic attack on the Cl ligand in the *trans* position to its electrophilic site (Fig. 1). The alignment of the dipole moments of $[\{Mo_6Cl_8^i\}Cl_5^a\square^a]^-$ ions (6.52 Debye) with the electric field induces that the electrophilic sites and nucleophilic sites of two consecutive $[\{Mo_6Cl_8^i\}Cl_5^a\square^a]^-$ ions are positioned to avoid coulomb repulsion if interacting (Fig. 1).

Such superelectrophilic behaviors are reported for cations;[23] the only anions known to date are the $[B_{12}L_{11}]^-$ series which activate inert gas. Dimerization of $[B_{12}I_{11}]^-$ is the only anion–anion interaction known in the gas phase.[8–10] Herein, we demonstrate that such electrophilic behavior exists for $[\{Mo_6Cl_8^i\}Cl_5^a\square^a]^-$ and that it leads to an iono-covalent bond creation with another anion. The ideal molecular orientation induced by the alignment of the dipole moment and the applied electric field in the CID allows the electron-donating anions to interact without coulombic repulsion. Interestingly, $[\{Mo_6Cl_8^i\}Cl_5^a\square^a]^-$ ions have their nucleophile site in the *trans* position to its electrophilic site. This makes the $[\{Mo_6Cl_8^i\}Cl_5^a\square^a]^-$ ion a unique example in the inorganic chemistry of Janus anions exhibiting both nucleophilic and electrophilic character. This opens up a wide range of fundamental studies toward the activation of cluster units in the gas phase and further multi-reactivity. Functionalization of a surface by $[\{Mo_6Cl_8^i\}Cl_5^a\square^a]^-$ ions in a gas phase process becomes possible. It can provide for instance sensitive layers able to interact with volatile organic compounds for the design of antenna sensors such as some of us have recently patented.[24]

This work was granted access by the French HPC agency GENCI (TGCC/CINES/IDRIS – A0100800649/AD010800649R1). The authors warmly thank Rémi Marchal for technical support.

Conflicts of interest

There are no conflicts to declare.

Notes and references

1 N. T. K. Nguyen, C. Lebastard, M. Wilmet, N. Dumait, A. Renaud, S. Cordier, N. Ohashi, T. Uchikoshi and F. Grasset, *Sci. Technol. Adv. Mate.*, 2022, **23**, 547–578.
2 K. Kirakci, M. A. Shestopalov and K. Lang, *Coord. Chem. Rev.*, 2023, **481**, 215048.
3 A. Pinkard, A. M. Champsaur and X. Roy, *Acc. Chem. Res.*, 2018, **51**, 919–929.
4 P. Jena and Q. Sun, *Chem. Rev.*, 2018, **51**, 5755–5870.
5 A. W. Castleman and S. N. Khanna, *J. Phys. Chem. C*, 2009, **113**, 2664–2675.
6 P. Su, Z. Warneke, D. Volke, M. F. Espenship, H. Hu, S. Kawa, K. Kirakci, R. Hoffmann, J. Laskin, C. Wiebeler and J. Warneke, *J. Am. Soc. Mass Spectrom.*, 2023, **34**, 161–170.
7 V. K. Kochnev, V. V. Avdeeva, E. A. Malinina and N. T. Kuznetsov, *Russ. J. Inorg. Chem.*, 2014, **59**, 1268–1275.
8 M. Rohdenburg, M. Mayer, M. Grellmann, C. Jenne, T. Borrmann, F. Kleemiss, V. A. Azov, K. R. Asmis, S. Grabowsky and J. Warneke, *Angew. Chem., Int. Ed.*, 2017, **56**, 7980–7985.
9 M. Mayer, V. van Lessen, M. Rohdenburg, G. L. Hou, Z. Yang, R. M. Exner, E. Apra, V. A. Azov, S. Grabowsky, S. S. Xantheas, K. R. Asmis, X. B. Wang, C. Jenne and J. Warneke, *Proc. Natl. Acad. Sci. U. S. A.*, 2019, **116**, 8167–8172.
10 M. Rohdenburg, V. A. Azov and J. Warneke, *Front. Chem.*, 2020, **8**, 580295.
11 M. M. Zhong, H. Fang, Deepika and P. Jena, *Phys. Chem. Chem. Phys.*, 2021, **23**, 21496–21500.
12 K. Morokuma, *J. Chem. Phys.*, 1971, **55**, 1236.
13 K. Kitaura and K. Morokuma, *Int. J. Quantum Chem.*, 1976, **10**, 325–340.
14 T. Ziegler and A. Rauk, *Theor. Chim. Acta*, 1977, **46**, 1–10.
15 T. Ziegler and A. Rauk, *Inorg. Chem.*, 1979, **18**, 1755–1759.
16 T. Ziegler and A. Rauk, *Inorg. Chem.*, 1979, **18**, 1558–1565.
17 M. Raupach and R. Tonner, *J. Chem. Phys.*, 2015, **142**(1–14), 194105.
18 R. G. Parr and W. T. Yang, *J. Am. Chem. Soc.*, 1984, **106**, 4049–4050.
19 J. Warneke, T. Dulcks, C. Knapp and D. Gabel, *Phys. Chem. Chem. Phys.*, 2011, **13**, 5712–5721.
20 T. S. Zhao, J. Zhou, Q. Wang and P. Jena, *J. Phys. Chem. Lett.*, 2016, **7**, 2689–2695.
21 A. G. Harrison, *Rapid Commun. Mass Spectrom.*, 1999, **13**, 1663–1670.
22 C. M. Lock and E. W. Dyer, *Rapid Commun. Mass Spectrom.*, 1999, **13**, 422–431.
23 D. A. Klumpp and M. V. Anokhin, *Molecules*, 2020, **25**(1–25), 3281.
24 A. Denis, D. Rondeau, M. Himdi, X. Castel and S. Cordier, Antennas having ion cluster type sensors, WO2021/175796A1 (PCT/EP2021/055080), 2021.

